THE JOURNAL OF DERMATOLOGY

doi: 10.1111/1346-8138.12360

Journal of Dermatology 2014; **41**: 1–2

LETTER TO THE EDITOR

Calcification of the placenta in a woman with pseudoxanthoma elasticum with a mutation of the *ABCC6* gene

Dear Editor,

A 26-year-old woman was referred to our department from an obstetrician at 12 weeks of gestation for evaluation of non-symptomatic yellowish papules on the neck and axillae, which appeared at the age of 20 years (Fig. 1a). Histological examination of a yellow papule on the right axilla showed a band of eosinophilic granular material in the dermis. Elastica van Gieson stain showed fragmentation and clumping of elastic

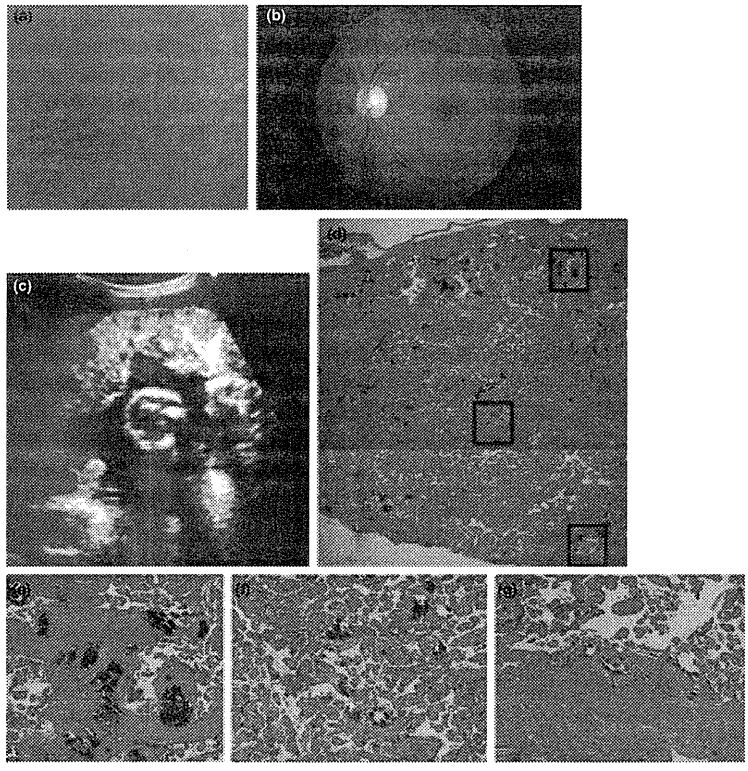

Figure 1. (a) Clinical presentation of yellow papules on the right axilla. (b) Fundus photograph of the patient's left eye. Whereas angioid streaks were observed around the optic disc and peau d'orange fundus was apparent temporal to the macula, no choroidal neovascularization was detected. (c) An echogram of the uterus at the 35th week detected calcification of the placenta. (d) Histological examination showed multiple calcified lesions in the placenta (hematoxylin–eosin [HE], ×12.5). The upper and lower parts were the fetal and maternal side of the placenta, respectively. (e) Calcification in chorion frondosum. High magnification of upper black box in (d) (fetal side) (HE, ×100). (f) Calcification in the villus. High magnification of middle black box in (d) (HE, ×100). (g) High magnification of the placenta in lower black box in (d) showed calcification of blood vessels in the decidua basalis (maternal side of the placenta) (HE, ×100).

Correspondence: Atsushi Utani, M.D., Ph.D., Department of Dermatology, Graduate School of Medicine, Nagasaki University, Nagasaki 606-8507, Japan. Email: utani@nagasaki-u.ac.jp

Author contribution: Drs Tanioka and Utani had full access to all of the data in the study and take responsibility for the integrity of the data and the accuracy of the data analysis. Study concept and design: Tamura, Kondo. Acquisition of data: Konishi, Yomisura. Analysis and interpretation of data: Utani, Tanioka, Kondo, Tamura. Drafting of the manuscript: Tanioka. Critical revision of the manuscript for important intellectual content: All authors. Statistical analysis: None. Administrative, technical, or material support: None. Study supervision: Miyachi, Konishi, Yoshimura.

Financial disclosure: None reported.

Approval: This study was approved by the local institutional review board.

fibers, where calcification of the degenerated fibrous components was revealed by von Kossa stain. Sequencing of the *ABCC6* gene detected a heterozygous mutation of C595T (nonsense mutation Q199X).

These skin lesions were diagnosed as pseudoxanthoma elasticum (PXE); thereafter, the other signs of PXE were screened by consulting specialists. Fundoscopic examination detected angioid streaks in both eyes, regardless of having no visual disturbance (Fig. 1b).

Electrocardiogram and echogram of the heart showed no abnormality and no calcification of large blood vessels.

At 30th week of pregnancy, a prenatal ultrasonography detected severe calcification of the placenta (Fig. 1c).

She delivered a healthy baby boy weighing 2810 g vaginally at the 39th week. The placenta (17 cm × 21 cm × 2.5 cm) weighed 640 g, and had grossly visible calcification. The calcification of vessels was evident not only in the decidua basalis (maternal side of the placenta) but also in the villus and the chorion frondosum (fetal side) (Fig. 1d–g). The umbilical arteries and vein showed slight blood congestion, but no calcification.

Pregnancy in PXE has been described to have severe complications, leading health-care providers to advise women with PXE against becoming pregnant. However, a study of 407 patients with PXE showed that it is not associated with markedly increased fetal loss or adverse reproductive outcomes.[1] On the other hand, a paper pointed out the risk on ocular lesions by labor and delivery.[2] Obstetric prognosis is dependent on the vascular damage caused by PXE. In the present case, screening examination could not find any vascular abnormalities.

The mechanism of calcification is speculated to be an abnormal function of calcium metabolism, because *ABCC6* is supposed to code a membrane transport protein.[3] Its substrate is still unknown, but is probably an organic anion, which prevents calcification in the body. We speculated that the putative factor, which prevents calcification, is missing in patients with PXE. Q199X is the second commonest mutation in Japanese patients with PXE. Ten out of 70 Japanese patients with PXE have this nonsense mutation.

Calcification is often found in the maternal side of the mature placenta even in women with non-PXE, while villous calcification is uncommon.[4] Calcification was much more pronounced in PXE than in controls in all placental regions; maternal side, villi and fetal side.[5] Also, in the present case, the calcification was more severe in the maternal side than in the fetal side.

The diagnosis of PXE is often difficult, however, skin lesions are the first indication of PXE, which usually appears during the first and second decade of life. Dermatological evaluation of a woman with severe calcification of the placenta may lead to a diagnosis of PXE.

CONFLICT OF INTEREST: None declared.

Miki TANIOKA,[1] Atsushi UTANI,[2] Hiroshi TAMURA,[3] Nagahisa YOSHIMURA,[3] Norihito KASHIWAGI,[4] Eiji KONDO,[5] Ikuo KONISHI,[5] Yoshiki MIYACHI[1]

[2]*Department of Dermatology, Nagasaki University Graduate School of Medicine, Nagasaki,* [1]*Departments of Dermatology,* [3]*Ophthalmology,* [4]*Department of Obstetrics and Gynecology, Kashiwagi Clinic, and* [5]*Obstetrics and Gynecology, Kyoto University Graduate School of Medicine, Kyoto, Japan*

REFERENCES

1 Bercovitch L, Leroux T, Terry S, Weinstock MA. Pregnancy and obstetrical outcomes in pseudoxanthoma elasticum. *Br J Dermatol* 2004; **151**: 1011–1018.
2 Farhi D, Descamps V, Picard C *et al.* Is pseudoxanthoma elasticum with severe angioid streaks an indication for Caesarean section? *J Eur Acad Dermatol Venereol* 2006; **20**: 1328–1399.
3 Li Q, Uitto J. Heritable ectopic mineralization disorders: the paradigm of pseudoxanthoma elasticum. *J Invest Dermatol* 2012; **132**: E15–E19.
4 Ramos-e-Silva M, Li'bia Cardozo Pereir A, Oliveira G *et al.* Connective tissue diseases: pseudoxanthoma elasticum, anetoderma, and Ehlers-Danlos syndrome in pregnancy. *Clin Dermatol* 2006; **24**: 91–96.
5 Gheduzzi D, Taparelli F, Quaglino D *et al.* The placenta in pseudoxanthoma elasticum: clinical, structural and immunochemical study. *Placenta* 2001; **22**: 580–590.

ORIGINAL ARTICLE

An *Ex Vivo* Model Employing Keloid-Derived Cell–Seeded Collagen Sponges for Therapy Development

Yosuke Yagi[1,2,6], Eri Muroga[1,6], Motoko Naitoh[3], Zenzo Isogai[4], Seiya Matsui[1,5], Susumu Ikehara[2], Shigehiko Suzuki[3], Yoshiki Miyachi[1] and Atsushi Utani[2]

The most distinctive feature of keloid is the extreme deposition of extracellular matrix, including collagens and proteoglycans (PGs). The focus of this study was the PG versican, which presumably defines keloid volume because of its ability to retain large amounts of water through its component glycosaminoglycans (GAGs). The excessive deposition of versican in keloids was examined by immunohistochemical analysis and by upregulation of the versican gene in these lesions by real-time PCR. The latter showed that mesenchymal cells derived from keloid lesion (KL) cells continue to exhibit above-normal versican production in culture. To establish a model of GAG deposition in keloids, collagen sponges seeded with KL cells (KL-SPos) were implanted in the subcutaneous space of nude mice. After 1 month, the KL-SPos were significantly heavier than the fibroblast (Fb)-seeded sponges (Fb-SPos). This *ex vivo* model was subsequently used to examine an inhibitory ability of IL-1β that was identified to reduce versican *in vitro*. IL-1β or chondroitinase ABC, when injected directly, successfully reduced the weight of the KL-SPos. Thus, on the basis of the change in weight of the seeded sponges, this *ex vivo* model can be used to test therapies aimed at reducing or inhibiting keloid formation and to study the pathogenesis of this aberrant response.

Journal of Investigative Dermatology (2013) **133,** 386–393; doi:10.1038/jid.2012.314; published online 6 September 2012

INTRODUCTION

Keloids occur spontaneously or following minor trauma, expanding beyond the boundaries of the original wound and causing serious functional and cosmetic problems. In people predisposed to keloid development, normal wound-healing processes are derailed, leading to an exuberant cellular response that includes excessive extracellular matrix (ECM) production and deposition (Wolfram *et al.*, 2009).

Our group (Naitoh *et al.*, 2005), as well as others (Smith *et al.*, 2008), determined that ECMs are overexpressed in keloid tissues and cells, respectively, using microarray assays. Recently, we demonstrated that micro-RNA-mediated mechanisms, namely a significant decrease in the level of miR196, was involved in the increased collagen synthesis characteristic of keloids (Kashiyama *et al.*, 2012). In addition, we showed that in these lesions, elastic fiber formation is disrupted because of the excess amounts of the glycosaminoglycan (GAG), chondroitin sulfate (CS), and dermatan sulfate (DS) (Ikeda *et al.*, 2009).

Versican is a member of the CS/DS-proteoglycan (PG) family. It is distributed in a variety of soft tissues and participates in cell adhesion, migration, proliferation, differentiation, and cartilage development (Wu *et al.*, 2005; Matsumoto *et al.*, 2006).

The sulfate or carbonyl moieties that form the long GAG side chains of versican enable it to hold large amounts of water. As excessive PG deposition contributes significantly to keloid volume, the elimination of these molecules by targeted treatment would significantly contribute to resolving the clinical problems associated with keloid development. Currently, international clinical recommendations on scar management, including keloids, comprise several treatment modalities (Mustoe *et al.*, 2002). However, among these, triamcinolone, surgery, radiation, and combination therapy have been shown to actually promote the recurrence of keloids rather than permanently eliminate them (Al-Attar *et al.*, 2006; van de Kar *et al.*, 2007; Butler *et al.*, 2008). The difficulty in developing a successful therapeutic strategy is further complicated by the absence of an appropriate model of keloids, a refractory disorder that is specific to humans.

The GAG deposition model of keloids developed in this study was based upon our observation of increased versican

[1]*Department of Dermatology, Graduate School of Medicine, Kyoto University, Kyoto, Japan;* [2]*Department of Dermatology, Graduate School of Medicine, Nagasaki University, Nagasaki, Japan;* [3]*Plastic Reconstructive Surgery, Graduate School of Medicine, Kyoto University, Kyoto, Japan;* [4]*Department of Dermatology, National Center for Geriatrics and Gerontology, Aichi, Japan and* [5]*Drug Discovery Research Laboratories, Maruho Co., Ltd., Kyoto, Japan*

[6]*These authors contributed equally to this work.*

Correspondence: Atsushi Utani, Department of Dermatology, Graduate School of Medicine, Nagasaki University, 1-7-1 Sakamoto, Nagasaki 852-8501, Japan. E-mail: utani@nagasaki-u.ac.jp

Abbreviations: CS, chondroitin sulfate; DS, dermatan sulfate; ECM, extracellular matrix; Fb, fibroblast; GAG, glycosaminoglycan; KL, keloid lesion; PG, proteoglycan; RT-PCR, real-time PCR

Received 8 March 2012; revised 20 June 2012; accepted 9 July 2012; published online 6 September 2012

transcription in primary cultured keloid cells, as determined in promoter assays. Sponges seeded with these aberrant cells were implanted into the subcutaneous space of nude mice and were used to study the inhibitory effect of several compounds. Of the cytokines and growth factors tested, only IL-1β inhibited versican expression. Thus, this animal model provides an invaluable approach to the development of effective therapies aimed at reducing keloid formation, which can then be tested in human trials. Furthermore, it can be used to identify the *in vivo* components that promote ECM formation in these abnormal tissues.

RESULTS

Versican accumulation and upregulation of the gene in keloids

In a previous study (Ikeda *et al.*, 2009), we found that the ECM deposited in keloids contains large amount of CS and DS. Microarray assays analyzing these tissues showed that versican and other PGs comprising the ECM were expressed at higher levels than in nonlesional skin (Naitoh *et al.*, 2005). To confirm that versican is expressed at aberrantly high levels in keloids, we subjected six samples of keloids (K1–K6) to histopathological analysis. Hematoxylin–eosin staining revealed numerous fibrillar collagenous matrices forming a whorled pattern and a central collection of broad, compact, hyalinized, and collagenous bundles (Figure 1a). The presence of massive amounts of GAGs in these matrices was evidenced by toluidine blue staining (Figure 1a). Immunohistochemical analysis with anti-versican antibody demonstrated intense versican deposition in the keloids, but not in nonlesional skin (Figure 1a). However, there was no difference in hyaluronan accumulation (Figure 1a). These observations suggest that versican is a specific marker of keloids.

Alternative splicing produces several versican isoforms, designated V0–V3 (Wu *et al.*, 2005). Two major versican transcripts, namely the V0 and V1 isoforms, were detected in both normal human skin and in keloids by real-time PCR (RT-PCR) analysis (data not shown). RT-PCR analysis of the three keloid-derived RNAs and the three normal skin–derived RNAs revealed substantially higher versican mRNA levels in keloids than in normal skin (Figure 1b). Semiquantitative RT-PCR of the six keloid-derived RNAs (K1–K6) and the RNAs derived from five normal skin samples (N1–N5) showed a similar tendency (data not shown).

Primary cultured cells derived from keloids continue to overexpress PGs

Eight keloid cell lines (keloid lesion (KL) cells) were established from eight individuals and eight normal fibroblast (Fb) lines were established from another eight. Microarray analysis of the ECM using KL and Fb cell line showed that the former continued to overexpress ECM, and showed upregulation of three PGs (versican, aggrecan, and lumican) under the

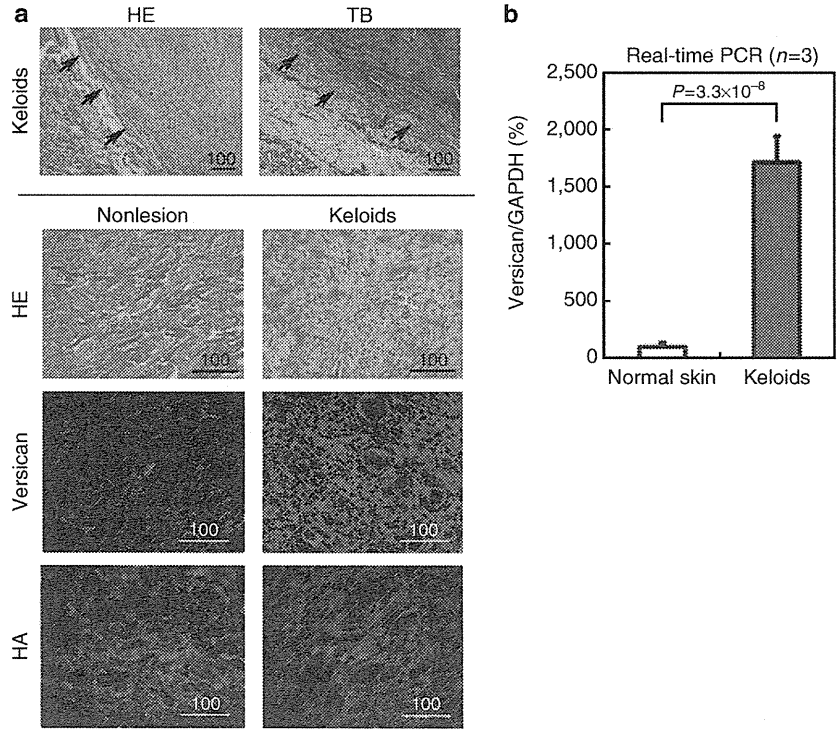

Figure 1. Versican accumulation and upregulation in keloids. (**a**) Hematoxylin–eosin (HE) staining revealed the deposition of an abnormal fibrillar collagenous matrix within the keloids. Toluidine blue (TB) staining at pH 2.5 showed metachromasia, indicative of glycosaminoglycan accumulation in the keloids. Arrows point to the boundary of the lesion. The keloids contained large deposits of versican, but there was no increase in hyaluronan (HA) levels. Representative images of the keloids obtained from six individuals are shown. Bar = μm. (**b**) Real-time PCR analysis of versican mRNA expression in samples of normal skin and of keloids. Mean ± SD and versican/glyceraldehyde 3-phosphate dehydrogenase ratios are shown.

Table 1. Microarray analysis of upregulated ECM genes in KL cells

Gene	Protein	mRNA KL cells /mRNA Fb[1]
COL10A1	Collagen α1 (X)	10.4
COL2A1	Collagen α1 (II)	10.3
ACAN	Aggrecan	6.2
COL9A1	Collagen α2 (IX)	3.9
COL11A1	Collagen α1 (XI)	3.6
LUM	Lumican	3.4
COL8A1	Collagen α1 (VIII)	2.8
VCAN	Versican	2.5
THBS1	Thrombospondin 1	2.4
COL17A1	Collagen α1 (XVII)	2.2
COL9A3	Collagen α3 (IX)	2.1

Abbreviations: ECM, extracellular matrix; Fb, fibroblast; KL, keloid lesion.
[1]Determined by microarray analysis performed in the current study.

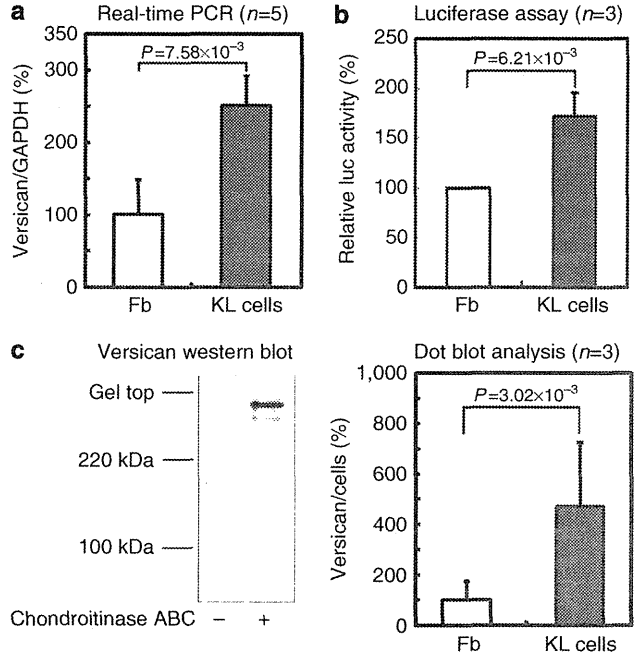

Figure 2. Versican upregulation in cultured keloid lesion (KL) cells. (**a**) KL cells and fibroblasts (Fbs) were analyzed for versican expression by real-time PCR. Versican/glyceraldehyde 3-phosphate dehydrogenase (GAPDH) ratios were calculated by setting the versican mRNA expression of one Fb cell line at 100%. The mean ± SD and the versican/GAPDH ratios are shown. (**b**) Both cells were transfected with a versican promoter luciferase reporter construct containing the versican promoter region (−559 to +353) and part of exon 1 fused to the luciferase gene. Luciferase activity was measured in quadruplicate and was calculated by setting the luciferase activity of one Fb cell line at 100%. Shown are the mean luciferase activities ± SD. (**c**) The antibody 2B1 specifically bound to versican (around 450 kDa). Dot-blot analysis of versican protein in conditioned medium.

culture conditions used (Table 1); all three PGs are upregulated in tissues (Naitoh *et al.*, 2005).

Upregulation of versican expression in KL cells

To determine whether versican is specifically upregulated in primary cultured KL cells, versican mRNA levels were measured. As shown by RT-PCR, the ratio of versican to glyceraldehyde 3-phosphate dehydrogenase expression in KL cells was 2.54 ± 0.53-fold higher than that in Fbs ($n = 5$ for both KL cells and Fbs) (Figure 2a). Furthermore, we used luciferase reporter assays to examine the activity of the versican promoter region, spanning −559 to +353, in KL cells and Fbs. As shown in Figure 2b, luciferase activity was 1.73 ± 0.22-fold higher in KL cells. After confirming that antibody 2B1 specifically bound to versican, we performed dot-blot analysis, which showed that KL cells overproduce versican protein (4.71 ± 2.53-fold higher than Fbs; Figure 2c).

Regulation of versican expression

Hypothesizing that a decrease in versican expression would lead to a corresponding reduction in keloid volume, we screened various cytokines, growth factors, and signaling pathway inhibitors. We carried out a series of studies in which LY294002, SB202190, and PD98059 were used to inhibit the PI3K, p38 MAPK, and ERK pathways, respectively. The results showed that PI3K and p38 MAPK, but not ERK, stimulated versican expression in both KL cells and Fbs (Figure 3a).

Among the growth factors and cytokines tested. The addition of IL-1β to Fbs and KL cells reduced versican expression in both, by 49.6 ± 13% and 21.2 ± 3.3%, respectively, compared with the corresponding untreated cells (Figure 3b). These results are consistent with other studies in which IL-1β reportedly suppressed versican expression in gingival Fbs (Qwarnstrom *et al.*, 1993) and arterial smooth muscle cells (Lemire *et al.*, 2007). Exogenous IL-1β also suppressed relative promoter activity in Fbs and KL cells, as evidenced by a decrease in luciferase activity of 65.8 ± 6.9% and 36.5 ± 10%, respectively (Figure 3c).

We then examined whether differences in the expression of IL-1β and IL-1 receptors by KL cells and Fbs accounted for the differential response to IL-1β and thus for the upregulation of versican in KL cells. ELISA assays showed that the amounts of endogenous IL-1β protein in the conditioned medium of both cell types were below the detectable limit (data not shown). Furthermore, according to RT-PCR, KL cells and Fb contain similar levels of IL-1 receptor mRNA (data not shown). Finally, the addition of an IL-1 receptor antagonist did not affect versican expression, although it completely blocked IL-1β-induced versican downregulation (Figure 3d). These results indicate that endogenous IL-1β is not involved in versican gene regulation under these experimental conditions.

Generation of an *ex vivo* GAG deposition model in mice

As noted above, keloid formation occurs only in humans, and thus there is no appropriate animal model. We therefore sought to establish an *ex vivo* model using the ECM-overproducing KL cells. In a previous study, we found that

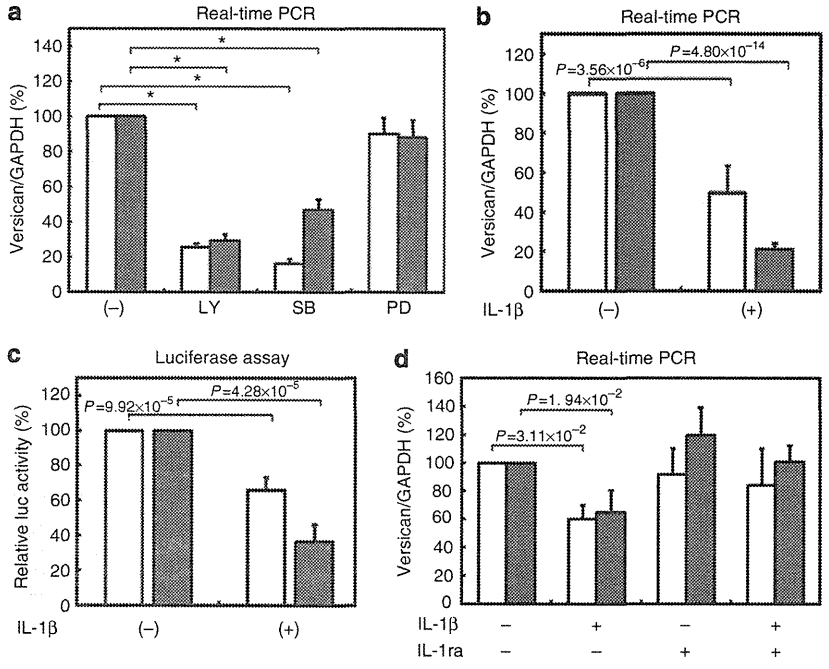

Figure 3. Analysis of signaling pathways and the effects of IL-1β on versican expression *in vitro*. (**a**) In keloid lesion (KL) cells (closed column) and fibroblasts (Fbs) (blank column), PI3K was blocked by the addition of LY294002 (LY), p38 MAPK by SB202190 (SB), and ERK by PD98059 (PD). *$P<0.001$. (**b**) KL cells or Fbs were treated with IL-1β. (**c**) Transfection was carried out 48 hours before stimulation of the cells with IL-1β (20 U ml^{-1}). (**d**) Both cell types were treated with recombinant IL-1 receptor antagonist and/or IL-1β. Versican/glyceraldehyde 3-phosphate dehydrogenase (GAPDH) ratios or luciferase promoter activity was calculated by setting the value obtained from the untreated KL cells or Fb at 100%. All experiments were performed in triplicate. Representative data, expressed as the mean ± SD, are shown.

cartilage could be successfully reconstructed using a collagen sponge as a scaffold for chondroprogenitor cells (Togo *et al.*, 2006). Accordingly, these sponges, which consist of chemically cross-linked collagen resistant to collagenase digestion *in vivo*, were used in our *ex vivo* model. Collagen sponges were seeded with 5×10^5 KL cells (KL-SPos) or Fbs (Fb-SPos) and then implanted into the subcutaneous space of nude mice (Figure 4a). After various incubation periods, the KL-SPo and Fb-SPo were removed and weighed. After 1 month, the KL-SPos were less translucent (Figure 4a) and were significantly heavier than the Fb-SPos (29 ± 8.1 mg vs 17 ± 6.9 mg, respectively; Figure 4a). In contrast, a 3D *in vitro* incubation of KL-SPos and Fb-SPos for 1 month did not result in significant weight differences (Figure 4b). In sponges incubated subcutaneously for 1 month, hematoxylin–eosin and alcian blue staining, respectively, showed that greater amounts of ground substances and GAGs had been deposited in the KL-SPos than in the Fb-SPos (Figure 4c). Immunostaining evidenced larger amounts of versican, but not of hyaluronan (data not shown), in the KL-SPos than in the Fb-SPos (Figure 4d).

Injections with chondroitinase ABC or IL-1β reduced implant growth

The implants were treated with chondroitinase ABC to determine whether the weight increase in the KL-SPo could be suppressed by removing the CS/DS chains of PGs, including versican. Weekly injections of 0.5 U of chondroitinase ABC for 1 month caused a significant reduction in the weight of KL-SPo (from 26 ± 6.7 mg to 14 ± 6.8 mg; Figure 5a). In the KL-SPos, alcian blue staining revealed that the chondroitinase ABC injections had substantially reduced GAG deposition (Figure 5b), whereas versican immunostaining demonstrated that the enzymatic removal of the CS/DS chains caused a significant decrease in the levels of the core proteins of the PGs (Figure 5b). These data suggest that versican deposition in the KL-SPos is mediated by CS/DS-chain interactions with other matrix components. In contrast, the amount of collagen deposition in the injected KL-SPos and uninjected KL-SPos was essentially the same, as shown by Masson trichrome staining (Figure 5b).

As exogenous IL-1β reduced versican expression *in vitro*, we tested its effect on KL-SPos. Although there were no significant differences in alcian blue staining, Masson trichrome staining, and versican immunostaining between IL-1β-treated and nontreated sponges (data not shown), a significant reduction of weight was achieved with three-times-weekly injections of the cytokine (Figure 5c).

DISCUSSION

Although it is clear that normal wound-healing processes are derailed in individuals predisposed to developing keloids, the pathogenic mechanisms of keloids are poorly understood, including those resulting in excess ECM production (Wolfram *et al.*, 2009). PGs are expressed in large amounts in keloids

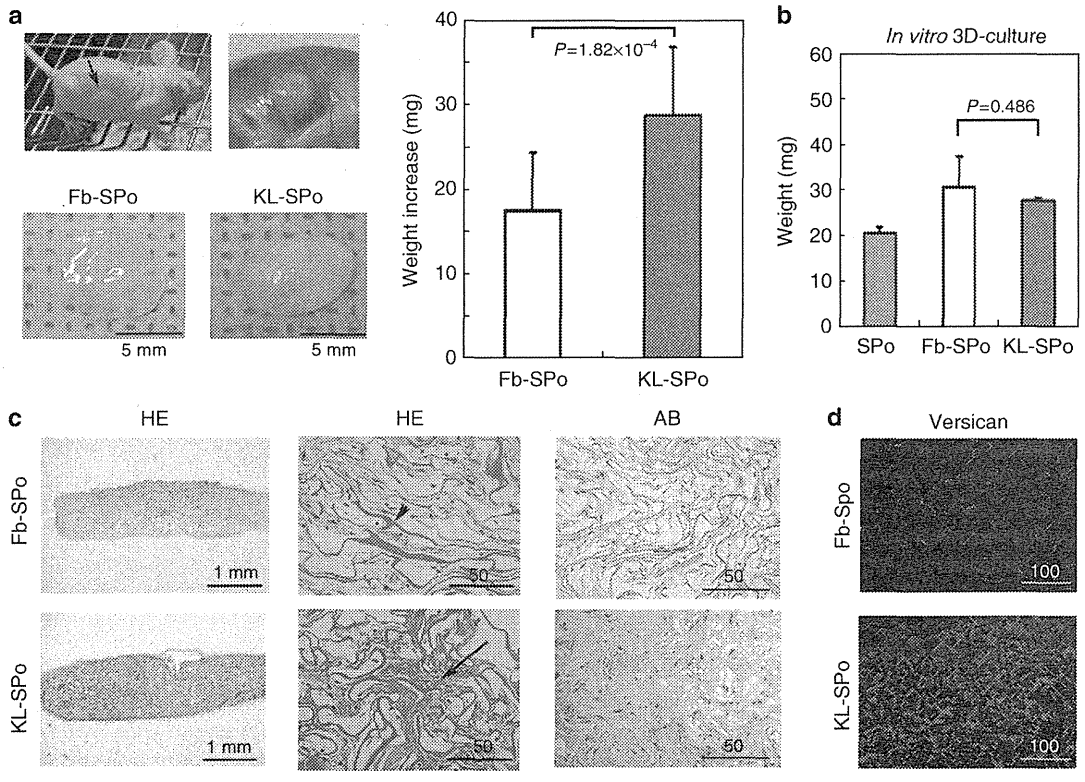

Figure 4. Generation of an *ex vivo* glycosaminoglycan deposition model in nude mice. (**a**) Collagen sponges seeded with keloid lesion (KL) cells (KL-SPos) or fibroblasts (Fb) (Fb-SPos) were implanted into the subcutaneous space of the mice (upper two images). After 1 month, the sponges were removed (lower two images). The mean ± SD of the increase in the weights of the sponges is shown. (**b**) SPo, Fb-SPo, and KL-SPo were cultured. The mean ± SD of the weights of samples is shown. (**c**) Sponges were stained with hematoxylin–eosin (HE), alcian blue (AB), and nuclear fast red. The arrowhead indicates the chemically cross-linked collagen fibers of the collagen sponges, and the arrow indicates the ground substance deposits. Bar = 1 or 50 μm. (**d**) Versican immunostaining of KL-SPos and Fb-SPos. Bar = 100 μm.

and, because of their GAG-mediated capacity to retain large amounts of water, are likely to have important roles in determining the volume of these aberrant tissues. We previously reported that the GAGs deposited in keloid tissues mainly consist of CS/DS (Ikeda *et al.*, 2009). Of the three PGs showing increased expression in keloids, lumican GAGs only carry keratan sulfate chains. Because the major GAG found in keloids is CS (Ikeda *et al.*, 2009), we ruled out lumican as one of the PGs whose level is increased in keloids. In our earlier study of keloids, we were unable to detect aggrecan expression by northern blotting; thus, we assumed its expressions to be weak in keloid tissue (Naitoh *et al.*, 2005). Therefore, we focused on versican as the major PG deposited in keloids.

Several groups have attempted to generate animal models of keloids (e.g., by implanting a piece of human keloid tissue into mice (Waki *et al.*, 1991; Polo *et al.*, 1998)); however, to date, they have not been widely used (Ramos *et al.*, 2008). Recently, hypertrophic scar tissue implanted into nude mice was shown to undergo a significant size reduction in response to the direct application of basic Fb growth factor (Eto *et al.*, 2012). However, we preliminarily tried to implant small pieces of keloid tissue into nude mice, but after 1 month, these pieces had undergone various degrees of size reduction, probably due to matrix degradation. It may be that size is a critical factor in the prolonged maintenance of the implanted tissue, which is influenced by the proper distribution of nutrients and/or oxygen from the surrounding tissue. In an earlier study, we succeeded in obtaining cartilage production in the subcutaneous space of nude mice by using a chemically cross-linked collagen sponge seeded with chondroprogenitor cells (Togo *et al.*, 2006). Accordingly, we speculated that these sponges would be an excellent material for studying the mechanisms of GAG deposition in keloids. Indeed, after 1 month, the KL-SPos were heavier than the Fb-SPos. This result in turn implied that the efficacy of test compounds in suppressing keloid volume could be estimated simply by weighing the sponges. Another advantage of the collagen sponges is that their elasticity facilitates injection with the various candidate therapeutic compounds. A sponge-like scaffold fabricated from polylactic acid (Chung *et al.*, 2008) was also tested, but it did not result in significant versican deposition (data not shown).

One of the aims of this study was to identify compounds that inhibited the growth of the KL-SPos. As TGF-β stimulates versican expression in dermal Fbs under *in vitro* conditions (Kahari *et al.*, 1991), blockade of the TGF-β signaling pathway may also be a potent candidate keloid-treatment modality. Similarly, it would be interesting to examine the

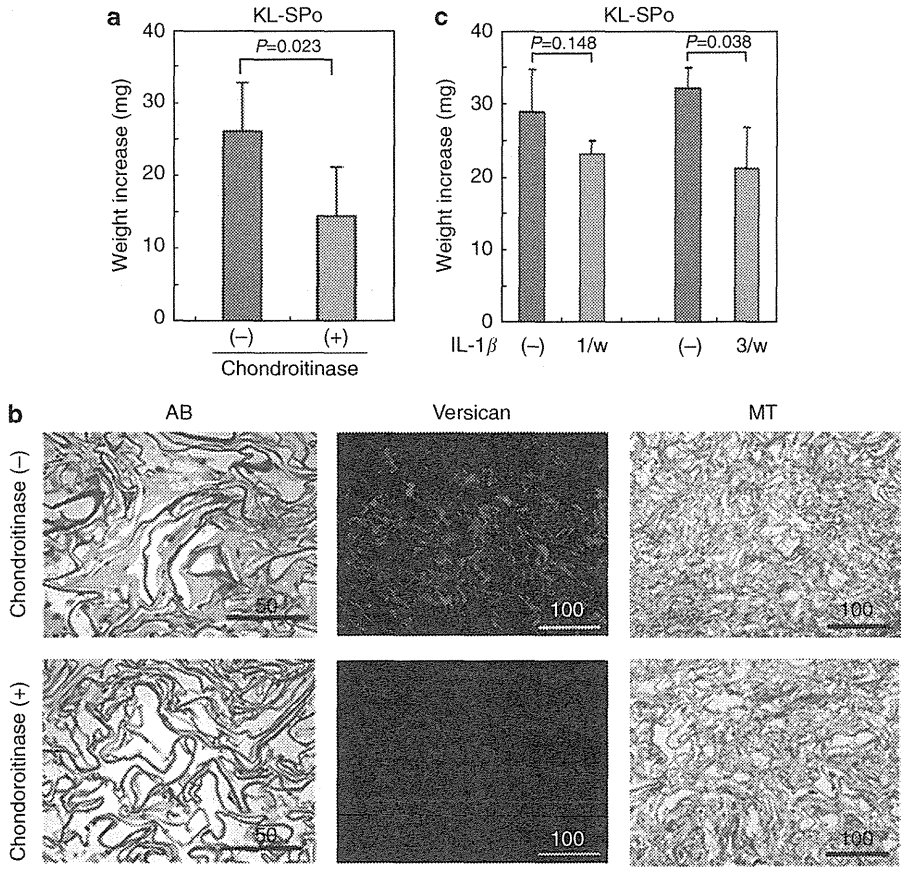

Figure 5. IL-1β injections reduce implant growth. (**a**) KL-SPos were transplanted into the subcutaneous space of nude mice. Chondroitinase ABC was injected into the sponges once a week for 1 month, starting 1 week post implantation. The sponges were then removed and immediately weighed. Shown are the mean ± SD implant weights of three animals per group (–): vehicle (0.1% BSA/H_2O). (**b**) Staining with alcian blue (AB) or Masson trichrome (MT), and immunostaining with anti-versican antibody of the chondroitinase ABC-treated (+) and -untreated (–) KL-SPos. Bar = μm. (**c**) IL-1β was injected into the sponges once or three times a week for 1 month, starting 1 week post implantation. Thrice-weekly injections significantly reduced the KL-SPo weight increase.

effects of PI3K and p38MAPK inhibitors on GAG deposition in our *ex vivo* system. Downregulation of versican deposition by IL-1β was observed in KL cells in our *ex vivo* model. Thus, IL-1β may be of therapeutic interest in keloids. Chondroitinase ABC may also be a potent inhibitor of keloid formation based on its ability to remove GAGs, as demonstrated in our *ex vivo* model. A reduction in keloid volume would be sufficient to relieve many of the clinical symptoms and cosmetic problems of affected individuals. Chondroitinase ABC is currently being tested in a phase III clinical trial in the USA and Japan for the treatment of interdisc herniation (http://www.seikagaku.co.jp/english/pdf/76.pdf). The results of that trial may be applicable to the treatment of keloids. Although there are currently several treatment modalities for keloids, many are unsatisfactory because they fail to prevent recurrence (Butler *et al.*, 2008). We developed a simple, reliable *ex vivo* model of keloids that can be used not only to evaluate novel anti-keloid agents but also to identify the mechanisms underlying the pathogenesis of keloids.

MATERIALS AND METHODS

Keloid samples and primary culture

Keloids are defined as raised, red, and inflexible scar tissue that invades the boundaries of the original wound (Butler *et al.*, 2008). Keloids and unaffected normal skin tissue specimens were obtained surgically with written informed consent, with adherence to the Declaration of Helsinki protocols, and with the approval of the Ethical Committee of the Kyoto University Medical School. Tissue samples were taken from keloids located on the shoulder, chest, or abdomen of six individuals (K1–K6, male:female ratio = 4:2; mean age = 36.3) and from normal skin tissue remaining after the surgical removal of benign tumors located on the face, buttock, abdomen, or inguinal region of five individuals (N1–N5, male:female ratio = 1:4; mean age = 31.6). All of the samples were subjected to histological examination and mRNA extraction.

Primary cultured cells were obtained from keloids located on the face, shoulder, chest, back, or abdomen of another eight individuals (male:female ratio = 6:2; mean age = 29.4) and from the normal skin of the face, forearm, buttock, or abdomen of eight additional individuals (male:female ratio = 5:3; mean age = 31.4). Primary cell

culture involved plating small pieces of excised keloid tissue on plastic dishes in 10% fetal bovine serum/DMEM with antibiotics and incubating the cultures at 37 °C until the cells grew out of the tissue pieces. These cells were maintained in the same culture medium and passaged by a 1:2–3 split when they reached early confluence.

For the signal inhibition assay, KL cells and Fbs were cultured in medium containing 30 μM LY294002 (PI3K inhibitor), 30 μM SB202190 (p38 MAPK inhibitor), or 20 μM PD98059 (ERK inhibitor; all from Calbiochem, Damstadt, Germany). For IL-1β signaling studies, the cells were cultured in the presence of IL-1β (20 U ml^{-1}; Roche Diagnostics, Indianapolis, IN). RNA was purified 15 hours after IL-1β treatment. Recombinant IL-1 receptor antagonist (0.5 μg ml^{-1}; R&D systems, Minneapolis, MN) was applied to both the KL cells and the Fbs 24 hours before RNA purification.

Animals and operations

The number of animals used in this study was kept to a minimum, and all possible efforts were made to reduce their suffering, in compliance with the protocols established by the Animal Research Committee of Kyoto University.

Immunohistochemistry

For versican immunostaining, mouse anti-human versican monoclonal antibody (2B1; from Seikagaku Kogyo, Tokyo, Japan) and Cy3-conjugated anti-mouse IgGs (Millipore-Chemicon, Billerica, MA) were used according to the manufacturer's instructions. For hyaluronan immunostaining, biotinylated hyaluronic acid-binding protein (Seikagaku Kogyo) and streptavidin-Cy3 (Sigma-Aldrich, St Louis, MO) were used according to the manufacturer's instructions. Fluorescence immunostaining was analyzed by confocal laser scanning microscopy using a Zeiss LSM 510 system (Carl Zeiss Microscopy, Göttingen, Germany).

RT-PCR

Total RNA was extracted and cDNA was synthesized as previously reported (Ikeda *et al.*, 2009). RT-PCR products were analyzed by quantitative RT-PCR by using TaqMan probe (Roche Applied Science, Mannheim, Germany), TaqMan Universal PCR Master Mix (Applied Biosystems, Carlsbad, CA), and the respective primers (Sigma-Aldrich) according to the manufacturer's instructions. Triplicate reactions were performed in an AB7300 real-time thermocycler (Applied Biosystems) under the following thermal cycles: 2 minutes at 50 °C, 1 minute at 95 °C, and 40 cycles of 15 seconds at 95 °C and 1 minute at 60 °C. The TaqMan probe and primers used were as follows: glyceraldehyde 3-phosphate dehydrogenase, probe no. 60, forward primer, (83–101 nt Genbank NM_002046.3) 5′-AGCCA CATCGCTCAGACAC-3′ and reverse primer (130–148 nt) 5′-GCCC AATACGACCAAATCC-3′; versican, probe no. 54, forward primer (9,657–9,675 nt Genbank NM_004385.3) 5′-GCACCTGTGTGCC AGGATA-3′ and reverse primer (9,703–9,726 nt) 5′-CAGGGATTA GAGTGACATTCATCA-3′; and IL-1 receptor, probe no. 60, forward primer (1,350–1,371 nt Genbank NM_000877.2) 5′-TGTTCATTTAT GGAAGGGATGA-3′ and reverse primer (1,403–1,427 nt) 5′-TTCTG CTTTTCTTTACGTTTTCATT-3′.

Transfection and luciferase assays

The promoter activity of KL cells and Fbs was assessed by inserting a −559 to +353 region of the human versican gene (GenBank U15963) (Naso *et al.*, 1994) upstream of the luciferase gene in the pTAL-luc plasmid (BD Biosciences Clontech, Palo Alto, CA). The construct was verified by DNA sequencing. KL cells or Fbs were seeded on 24-well plates at 1.5×10^5 cells per well and transfected with Fugene HD (Roche Applied Science) and their luciferase activities were measured with a Promega Dual Luciferase Reporter Assay kit (Promega, Madison, WI) according to the manufacturer's protocols.

Western and dot-blot analyses of versican protein

To collect conditioned medium, 2.0×10^5 KL cells or Fbs were seeded on six-well plates. Two days after serum starvation induced by culture in 2 ml of DMEM, conditioned medium was collected and used for western blot and dot-blot analyses, which were performed as described previously (Isogai *et al.*, 1996; Koyama *et al.*, 2007). Intensities of dots were calculated using ImageQuant TL (GE Healthcare, Amersham Place, UK). The values were expressed as the ratios to cell numbers.

Generation of an *ex vivo* GAG deposition model

Collagen sponges were prepared and were implanted into subcutaneous pockets of nude mice as previously reported (Togo *et al.*, 2006). Before implanting sponges, they were incubated overnight in 10% fetal bovine serum/DMEM with 5×10^5 KL cells or Fbs, thus generating KL-SPo and Fb-SPo, respectively. Four weeks after implantation, the KL-SPo and Fb-SPo were removed, weighed, and subjected to histological analysis as follows: after fixation with 10% phosphate-buffered formalin for 24 hours at 4 °C, the sponges were embedded in paraffin and sliced into 7.0-μm sections, which were either stained with hematoxylin–eosin or alcian blue (pH 2.5) or subjected to immunohistochemical analysis.

Injection of the collagen sponges with chondroitinase ABC and IL-1β

KL-SPos were injected once a week, starting 1 week post implantation, with *Proteus vulgaris* chondroitinase ABC (protease free: 0.1 U in 50 μl of 0.1% BSA/H_2O) or IL-1β (40 U in 20 μl of 0.1% BSA/phosphate-buffered saline). An equal amount of vehicle served as the control. At 4 weeks post implantation, the mice were killed and the sponges were removed and analyzed.

cDNA microarray analysis

Total RNA was isolated from cultured KL cells and Fbs using an RNeasy mini kit (Qiagen, Valencia, CA). Total RNA (1 μg) was amplified and labeled using the One-Cycle Target Labeling kit (Affymetrix, Santa Clara, CA).

Biotin-labeled cRNA (15 μg) was fragmented and hybridized to the GeneChip Human Genome U133 Plus 2.0 Array (Affymetrix). The array was incubated and signals were scanned according to the manufacturer's protocol. Expression profiles were analyzed based on the MAS5 algorithm using the GeneChip operating software (Affymetrix), with further analysis using GeneSpring 7.3 (Agilent Technologies, Palo Alto, CA). Raw intensity values from each chip were normalized to the 50th percentile of the measurements. Each gene was normalized to the median of that gene in the respective controls to enable the comparison of relative changes in gene expression levels between different conditions.

Statistical analysis

Student's *t*-test was used to examine differences between experimental groups. The data are expressed as the means ± SD. The calculated *P*-values were two-sided; $P<0.05$ was considered statistically significant.

CONFLICT OF INTEREST

The authors state no conflict of interest.

ACKNOWLEDGMENTS

We thank Dr Yoshihiko Yamada and Dr Kenneth Yamada, National Institute of Dental and Craniofacial Research, National Institutes of Health, for critical reading of the manuscript and their helpful suggestions. This work was supported in part by Grants-in-Aid (20591344 and 23659511) for Scientific Research from the Ministry of Education, Culture, Sports, Science and Technology of Japan, and by a grant from the Nakatomi Foundation to AU.

REFERENCES

Al-Attar A, Mess S, Thomassen JM *et al.* (2006) Keloid pathogenesis and treatment. *Plast Reconstr Surg* 117:286–300

Butler PD, Longaker MT, Yang GP (2008) Current progress in keloid research and treatment. *J Am Coll Surg* 206:731–41

Chung HJ, Steplewski A, Chung KY *et al.* (2008) Collagen fibril formation. A new target to limit fibrosis. *J Biol Chem* 283:25879–86

Eto H, Suga H, Aoi N *et al.* (2012) Therapeutic potential of fibroblast growth factor-2 for hypertrophic scars: upregulation of MMP-1 and HGF expression. *Lab Invest* 92:214–23

Ikeda M, Naitoh M, Kubota H *et al.* (2009) Elastic fiber assembly is disrupted by excessive accumulation of chondroitin sulfate in the human dermal fibrotic disease, keloid. *Biochem Biophys Res Commun* 390:1221–8

Isogai Z, Shinomura T, Yamakawa N *et al.* (1996) 2B1 antigen characteristically expressed on extracellular matrices of human malignant tumors is a large chondroitin sulfate proteoglycan, PG-M/versican. *Cancer Res* 56:3902–8

Kahari VM, Larjava H, Uitto J (1991) Differential regulation of extracellular matrix proteoglycan (PG) gene expression. Transforming growth factor-beta 1 up-regulates biglycan (PGI), and versican (large fibroblast PG) but down-regulates decorin (PGII) mRNA levels in human fibroblasts in culture. *J Biol Chem* 266:10608–15

Kashiyama K, Mitsutake N, Matsuse M *et al.* (2012) miR-196a downregulation increases the expression of type I and III collagens in keloid fibroblasts. *J Invest Dermatol* 132:1597–604

Koyama H, Hibi T, Isogai Z *et al.* (2007) Hyperproduction of hyaluronan in neu-induced mammary tumor accelerates angiogenesis through stromal cell recruitment: possible involvement of versican/PG-M. *Am J Pathol* 170:1086–99

Lemire JM, Chan CK, Bressler S *et al.* (2007) Interleukin-1 beta selectively decreases the synthesis of versican by arterial smooth muscle cells. *J Cell Biochem* 101:753–66

Matsumoto K, Kamiya N, Suwan K *et al.* (2006) Identification and characterization of versican/PG-M aggregates in cartilage. *J Biol Chem* 281:18257–63

Mustoe TA, Cooter RD, Gold MH *et al.* (2002) International clinical recommendations on scar management. *Plast Reconstr Surg* 110: 560–71

Naitoh M, Kubota H, Ikeda M *et al.* (2005) Gene expression in human keloids is altered from dermal to chondrocytic and osteogenic lineage. *Genes Cells* 10:1081–91

Naso MF, Zimmermann DR, Iozzo RV (1994) Characterization of the complete genomic structure of the human versican gene and functional analysis of its promoter. *J Biol Chem* 269:32999–3008

Polo M, Kim YJ, Kucukcelebi A *et al.* (1998) An *in vivo* model of human proliferative scar. *J Surg Res* 74:187–95

Qwarnstrom EE, Jarvelainen HT, Kinsella MG *et al.* (1993) Interleukin-1 beta regulation of fibroblast proteoglycan synthesis involves a decrease in versican steady-state mRNA levels. *Biochem J* 294(Part 2):613–20

Ramos ML, Gragnani A, Ferreira LM (2008) Is there an ideal animal model to study hypertrophic scarring? *J Burn Care Res* 29:363–8

Smith JC, Boone BE, Opalenik SR *et al.* (2008) Gene profiling of keloid fibroblasts shows altered expression in multiple fibrosis-associated pathways. *J Invest Dermatol* 128:1298–310

Togo T, Utani A, Naitoh M *et al.* (2006) Identification of cartilage progenitor cells in the adult ear perichondrium: utilization for cartilage reconstruction. *Lab Invest* 86:445–57

van de Kar AL, Kreulen M, van Zuijlen PP *et al.* (2007) The results of surgical excision and adjuvant irradiation for therapy-resistant keloids: a prospective clinical outcome study. *Plast Reconstr Surg* 119:2248–54

Waki EY, Crumley RL, Jakowatz JG (1991) Effects of pharmacologic agents on human keloids implanted in athymic mice. A pilot study. *Arch Otolaryngol Head Neck Surg* 117:1177–81

Wolfram D, Tzankov A, Pulzl P *et al.* (2009) Hypertrophic scars and keloids–a review of their pathophysiology, risk factors, and therapeutic management. *Dermatol Surg* 35:171–81

Wu YJ, La Pierre DP, Wu J *et al.* (2005) The interaction of versican with its binding partners. *Cell Res* 15:483–94

our data provide proof of concept support for targeting this molecule and its multi-cellular functions in psoriatic skin. Targeting VEGF topically may provide an effective new approach for treating mild-to-moderate psoriasis skin lesions by inhibiting angiogenesis and reducing leukocyte infiltration and KC proliferation.

Funding support

NLW is supported in part by grants from the National Institutes of Health (P30AR39750, P50AR05508, RO1AR063437; RO1AR062546) and the National Psoriasis Foundation.

Acknowledgments

The authors apologize to colleagues whose work could not be cited because of the space constraints. We thank Dr. John Rudge (Regeneron Pharmaceuticals, Tarrytown, NY) for providing VEGF-Trap and Dr. Thomas McCormick for feedback on the manuscript.

References

[1] Yancopoulos GD, Davis S, Gale NW, Rudge JS, Wiegand SJ, Holash J. Vascular-specific growth factors and blood vessel formation. Nature 2000;407:242–8.
[2] Kunstfeld R, Hirakawa S, Hong YK, Schacht V, Lange-Asschenfeldt B, Velasco P, et al. Induction of cutaneous delayed-type hypersensitivity reactions in VEGF-A transgenic mice results in chronic skin inflammation associated with persistent lymphatic hyperplasia. Blood 2004;104:1048–57.
[3] Jung K, Lee D, Lim HS, Lee S-I, Kim YJ, Lee GM, et al. Double anti-angiogenic and anti-inflammatory protein valpha targeting VEGF-A and TNF-alpha in retinopathy and psoriasis. J Biol Chem 2011;286:14410–18.
[4] Xia YP, Li B, Hylton D, Detmar M, Yancopoulos GD, Rudge JS. Transgenic delivery of VEGF to mouse skin leads to an inflammatory condition resembling human psoriasis. Blood 2003;102:161–8.
[5] Akman A, Yilmaz E, Mutlu H, Ozdogan M. Complete remission of psoriasis following bevacizumab therapy for colon cancer. Clin Exp Dermatol 2009;34:e202–4.
[6] Fournier C, Tisman G. Sorafenib-associated remission of psoriasis in hypernephroma: case report. Dermatol Online J 2010;16(17.).
[7] Wolfram JA, Diaconu D, Hatala DA, Rastegar J, Knutsen DA, Lowther A, et al. Keratinocyte but not endothelial cell specific overexpression of Tie2 leads to the development of psoriasis. Am J Pathol 2009;174:1443–58.
[8] Ward NL, Loyd CM, Wolfram JA, Diaconu D, Michaels CM, McCormick TS. Depletion of antigen-presenting cells by clodronate liposomes reverses the psoriatic skin phenotype in KC-Tie2 mice. Brit J Dermatol 2011;164:750–8.
[9] Schonthaler HB, Huggenberger R, Wculek SK, Detmar M, Wagner EF. Systemic anti-VEGF treatment strongly reduces skin inflammation in a mouse model of psoriasis. Proc Natl Acad Sci USA 2009;21264–69.

Doina Diaconu[a], Yi Fritz[a], Sean M. Dawes[a], Candace M. Loyd[a], Nicole L. Ward[a,b,*]
[a]*Department of Dermatology, Case Western Reserve University, Cleveland, OH 44106, USA;*
[b]*The Murdough Family Center for Psoriasis, University Hospitals Case Medical Center, Cleveland, OH 44106, USA*

*Corresponding author at: Case Western Reserve University, Department of Dermatology BRB519, 10900 Euclid Avenue, Cleveland, OH 44106, USA.
Tel.: +1 216 368 1111; fax: +1 216 368 0212
E-mail address: Nicole.ward@case.edu (N. Ward)

19 April 2013

http://dx.doi.org/10.1016/j.jdermsci.2013.08.005

Letter to the Editor

Co-existence of mutations in the *FBN1* gene and the *ABCC6* gene in a patient with Marfan syndrome associated with pseudoxanthoma elasticum

To the Editor,

Marfan's syndrome (MFS) is a disease with an autosomal dominant mode of inheritance that is manifested by characteristic skeletal abnormalities, including arachnodactyly, cardiovascular lesions (such as aortic dilatation), and ocular manifestations (such as ectopia lentis) [1]. The *FBN1* gene [2], which encodes fibrillin-1 (a component of elastic fibers), has been identified as the responsible gene. Pseudoxanthoma elasticum (PXE) is an autosomal recessive disorder that causes the ectopic mineralization of elastic fibers in soft connective tissues and mainly affects the eyes, skin, and cardiovascular system. The precise pathomechanisms of elastic fiber degeneration in PXE have not been fully elucidated despite a number of extensive studies [3]. The disease is linked to mutations in the ATP-binding cassette sub-family C member 6 (*ABCC6*) gene [4,5]. Here, we report the case of a patient who exhibited the clinical manifestations of both MFS and PXE and in whom pathological gene mutations were detected in both the *FBN1* gene and the *ABCC6* gene.

In 2003, a 64-year-old, tall Japanese woman presented with skin eruptions in her nuchal area, axillae, and groin. She had previously experienced angina pectoris and had undergone bypass surgery for coronary stenosis. The patient's family history revealed that her mother had been tall and had died of heart disease when the patient was a small child. A history and physical examination of her father revealed that he had no noteworthy clinical findings. The patient was the 5th of 5 siblings, and the eldest sister and the 4th sister had both been tall. The eldest sister had suddenly died of unknown causes in early childhood, and the 4th sister had died of aortic dissection. The patient had two children, a 38-year-old son and a 36-year-old daughter, and both had skeletal abnormalities that included a tall stature and arachnodactyly. Her son had undergone a Bentall operation for aortic dissection and aortic valve regurgitation as a child. Dermatological and ophthalmological examinations revealed no evidence of PXE in either child. The patient's family tree is shown in Fig. 1A.

At the time of the patient's initial examination, she was 165 cm tall and had an arm span of 185 cm. Dolichocephaly, pectus carinatum, disproportionately long limbs for her height, and arachnodactyly were noted (Fig. 1B). Numerous papules ranging in color from normal to yellow arrayed in a cobblestone pattern were observed in the nuchal area, axillae, and groin (Fig. 1C). Ophthalmological examinations revealed angioid streaks on her retinas. Radiography revealed linear calcifications in the upper limbs. The pathological findings for skin biopsy specimens from the affected sites consisted of clumps of fragmented basophilic fibers in the middle and lower layers of the dermis (Fig. 1D). Granular deposits that stained positive with von Kossa stain (Fig. 1E) were observed in specimens from the same sites.

A genomic DNA analysis of the patient's blood revealed a monoallelic nonsense mutation (c. 5454C > A: exon 44, p.Cys1818Stop) in the *FBN1* gene (Fig. 2A). Exon sequencing of *ABCC6* was performed using primers designed to eliminate *ABCC6* pseudogenes for exons 1–9 [6] and those designed by Prime 3 for

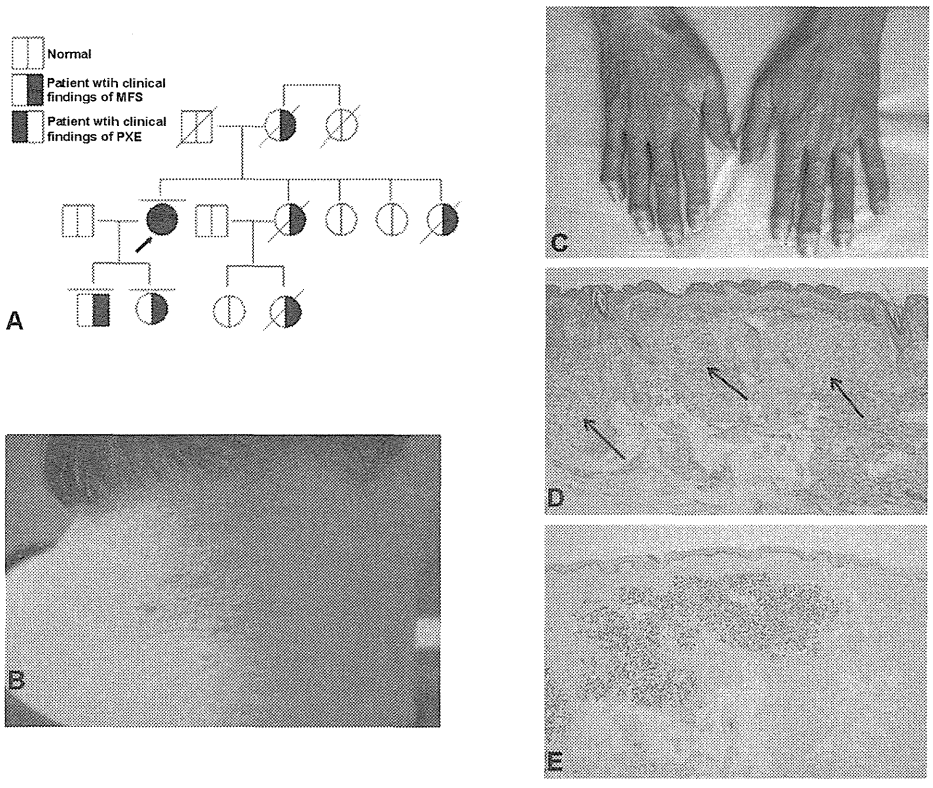

Fig. 1. Family tree, clinical findings, and pathological findings. (A) The patient's family tree. (B) Arachnodactyly. (C) Normal flesh color to yellow papules in a cobblestone pattern on the back of the patient's neck. (D) Clumps of fragmented basophilic fibers that look like thread waste are seen in the middle and lower layers of the dermis (hematoxylin and eosin, ×200). (E) Numerous granular deposits are seen among the clumps of fragmented fibers that have the appearance of thread waste (von Kossa stain, ×200).

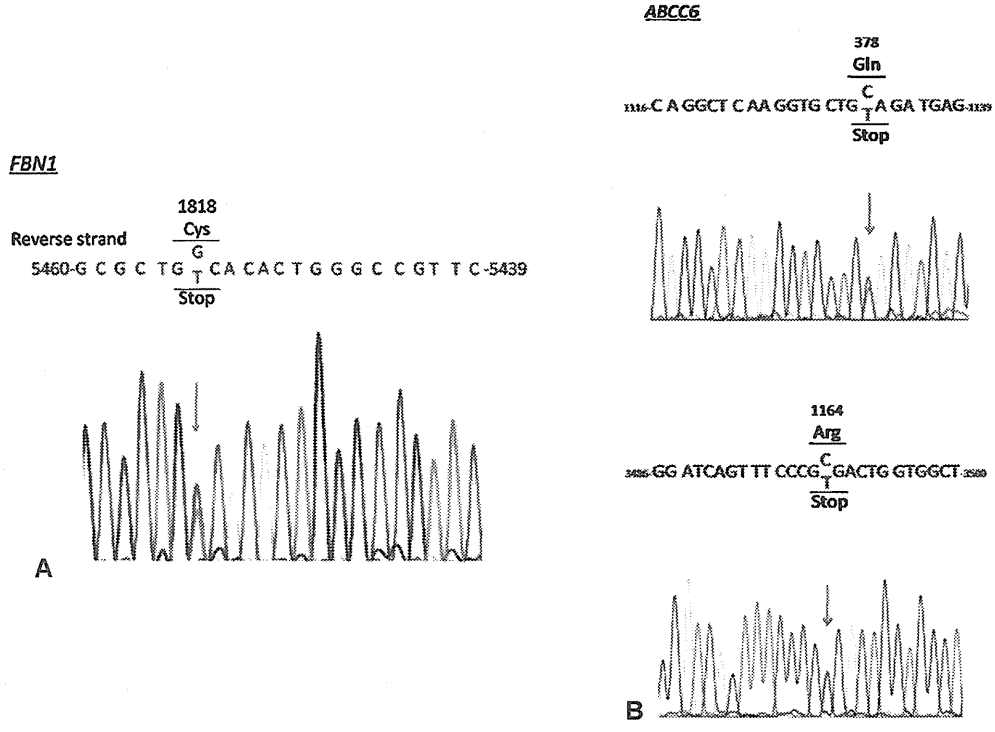

Fig. 2. Sequencing data of the patient's *FBN1* gene, which encodes fibrillin-1, and the *ABCC6* gene, which encodes ATP binding cassette C6 protein. (A) Sequence analysis of *FBN1*. A reverse sequence analysis of the portion of *FBN1* extending from c.5439 to c.5460 is shown. A monoallelic nonsense mutation (c.5454C > A, p.Cys1818Stop) was detected. (B) Sequence analysis of *ABCC6*. The results of sequence analyses of the portion of *ABCC6* extending from c.1116 to c.1139 and from 3486 to 3500 are shown. Compound heterozygous nonsense mutations (c.1132C > T, p.Gln378Stop and c.3490A > T, p.Arg1164Stop) were detected.

the other exons. The patient had two mutations in the ABCC6 gene: c.1132C > T in exon 9, p.Gln378Stop; and c.3490A > T in exon 24, p.Arg1164Stop (Fig. 2B). The patient's son had only the former mutation. Therefore, this patient had compound heterozygous nonsense mutations of *ABCC6*.

There has been one other report of a case of MFS and PXE in the same patient besides our own. The case was reported by Hidano et al. [7], similar to the present case, the previously reported patient was a member of a Japanese pedigree that exhibited the skeletal abnormalities associated with MFS, and the patient developed manifestations of both MFS and PXE. However, no search for gene mutations was performed in their case. Ours is the first report ever to describe MFS and PXE occurring in the same patient in whom mutations were confirmed in both the *ABCC6* gene and the *FBN1* gene. The concomitant presence of MFS and PXE seems to have been coincidental, but both conditions are hereditary diseases that give rise to elastic fiber abnormalities and to abnormalities in the same organs, including the cardiac blood vessels, and eyes. We plan to monitor the course of the presently reported patient to determine how her outcome compares with the outcome of patients who have only one of these diseases, either MFS or PXE.

References

[1] Burrows, Lovell CR. In: Tony B, Stephen B, Neil C, Christopher G, editors. Rook's textbook of dermatology. 7th ed., Oxford: Blackwell Science; 2004. p. 4621–31.
[2] Dietz HC, Cutting GR, Pyeritz RE, Maslen CL, Sakai LY, Corson GM, et al. Marfan syndrome caused by a recurrent de novo missense mutation in the fibrillin gene. Nature 1991;352:337–9.
[3] Uitto J, Li Q, Jiang Q. Pseudoxanthoma elasticum: molecular genetics and putative pathomechanisms. J Invest Dermatol 2010;130:661–70.
[4] Bergen AA, Plomp AS, Schuurman EJ, Terry S, Breuning M, Dauwerse H, et al. Mutation in *ABCC6* cause pseudoxanthoma elasticum. Nat Genet 2000;25:228–31.
[5] Lebwohl M, Neldner K, Pope FM, De Paepe A, Christiano AM, Boyd CD, et al. Classification of pseudoxanthoma elasticum. Report of a consensus conference. J Am Acad Dermatol 1994;30:103–7.
[6] Pulkkinen L, Nakano A, Ringpfeil F, Uitto J. Identification of *ABCC6* pseudogenes on human chromosome 16p: implications for mutation detection in pseudoxanthoma elasticum. Hum Genet 2001;109:356–65.
[7] Hidano A, Nakajima S, Shimizu T, Kimata Z. Pseudoxanthoma elasticum associated with Marfan syndrome. Ann Dermatol Venereol 1979;106:503–5.

Shujiro Hayashi[a], Atsushi Utani[b], Akira Iwanaga[b], Yosuke Yagi[b], Hiroko Morisaki[c], Takayuki Morisaki[c], Yoichiro Hamasaki[a], Atsushi Hatamochi[a,*]

[a]*Department of Dermatology, Dokkyo Medical University, School of Medicine, Mibu, Tochigi, Japan*;
[b]*Department of Dermatology, Graduate School of Biomedical Sciences Nagasaki University, Nagasaki-city, Nagasaki, Japan*;
[c]*Department of Bioscience and Genetics, National Cerebral and Cardiovascular Center Research Institute, Suita, Osaka, Japan*
*Corresponding author at: Department of Dermatology, Dokkyo Medical University, School of Medicine 880 Kitakobayashi, Mibu, Tochigi 321-0293, Japan.
Tel.: +81 282 87 2154;
fax: +81 282 86 3470
E-mail address: hatamo@dokkyomed.ac.jp (S. Hayashi)

22 April 2013

http://dx.doi.org/10.1016/j.jdermsci.2013.07.007

Letter to the Editor

Birth, life, and death of the MAGE3 hypothesis of alopecia areata pathobiology

Dear Editor,

In this distinguished journal, we routinely read discovery stories that have been ultimately crowned by success. Instead, here we would like to share our trials and tribulations along a less felicitous, yet very instructive and educational research journey that brought us close to what we hoped to be a clinically important advance in understanding the pathobiology of alopecia areata (AA), a tissue-specific, T cell-dependent autoimmune disease [1].

Most currently available evidence suggests that, upon interferon (IFN)-γ-induced collapse of the hair follicle's (HF's) physiological immune privilege (IP), as yet unidentified follicular autoantigens are exposed to preexisting autoreactive $CD8^+$ T cells by ectopically expressed major histocompatibility (MHC) class I molecules within the epithelium of anagen hair bulbs [1,2]. Peptides derived from melanogenesis-associated autoantigens expressed only by melanin-producing anagen HFs are persuasive candidates as key autoantigens in AA [3]. Therefore, focusing on well-investigated MHC class I-restricted melanocyte-related antigens known to be recognized by $CD8^+$ T cells is a sensible AA research strategy (supplementary text S1).

Supplementary material related to this article can be found, in the online version, at http://dx.doi.org/10.1016/j.jdermsci.2013.07.014.

We thus hypothesized that it should be possible to detect cytotoxic $CD8^+$ T cells (CTLs) directed against MHC class-I restricted autoantigens (tyrosinase, MAGE-A2, and MAGE-A3 (MBL)), using pentamer technology [4] (Supplemental text S2). To test this hypothesis, peripheral blood mononuclear cells (PBMCs) were obtained from Japanese healthy controls and AA patients (Supplementary Table S1).

Initially, this approach yielded auspicious results: MAGE-A3-reactive $CD8^+$ T cells were found to be significantly increased in PBMCs in the acute phase of AA with multifocal lesions (AAM) and alopecia areata totalis (AAT) compared to healthy controls, chronic phase of AAM, or AAT/alopecia areata universalis (AU) (Fig. 1a and Fig. S1a and b and Supplementary text S3) ($p = 0.025$ by Kruskal–Wallis ANOVA). Furthermore, skin infiltrating T cells of an acute phase AA lesion from one patient, which were isolated as previously described [5], also showed an increased number of MAGE-A3 specific CTLs (Fig. 1b) as that in peripheral blood nuclear cells (PBMCs) from the same AA patients (Fig. 1c) compared to the average frequency of MAGE-$A3^+$ T cells in PBMCs from control subjects (Fig. 1a). This pilot finding suggested an enrichment of MAGE-$A3^+$ CTLs in lesional AA skin.

Supplementary material related to this article can be found, in the online version, at http://dx.doi.org/10.1016/j.jdermsci.2013.07.014.

Next, we probed whether such CTLs can produce IFN-γ after stimulation with MAGE-A3 (supplementary text S4). Indeed, IFN-γ protein expression was significantly increased in $CD8^+$ T cells from acute phase AA patients co-cultured with MAGE-A3 compared to healthy controls (Fig. 1d and supplementary Fig. S1c and d). Moreover, the percentage of MAGE-A3 specific CTLs

皮膚病診療：35(9)：827～832, 2013

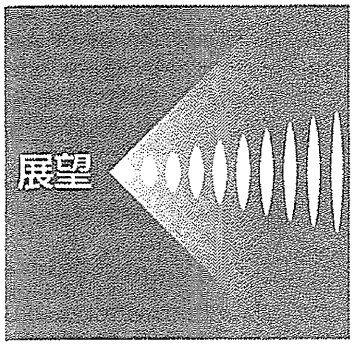

真皮マトリックス異常による全身疾患
——弾性線維性仮性黄色腫——

宇谷　厚志*

Key words
弾性線維，石灰化，虚血性疾患，網膜色素線条

はじめに

皮膚疾患の病変の多くは表皮にあり，真皮はそこに存在する血管，付属器などに炎症などがある場合に注目される．真皮の大部分を占める細胞外基質(細胞外マトリックス，extracellular matrix：ECM)は強固な構造を有し内臓を外界から保護する役割を担う．真皮細胞外マトリックスのうち，圧迫，ひっぱり，ねじれへの抵抗力を膠原線維が，変形からの復元を弾性線維が，そして水分を大量に保持できることでクッションの役割をグリコサアミノグリカンが担っている．真皮細胞外マトリックス異常から全身疾患をみつけるという今回のテーマに合致するのは，膠原線維の病的増加による強皮症，ガドリニウムと関連するとされる腎性全身性線維症，タキサン系抗癌剤による線維症などがある．また，膠原線維質の変化では遺伝性疾患(Ehlers-Danlos症候群など)がある．グリコサアミノグリカンが真皮に異常沈着する疾患として，糖尿病性浮腫性硬化症，甲状腺機能亢進による前脛骨粘液水腫，甲状腺機能低下による粘液水腫，マクログロブリン血症にみられる硬化性粘液水腫，浮腫性硬化症などが知られている．また膠原病(紅斑性ループス，皮膚筋炎など)の病変部の真皮で増加していることもあるので注意が必要である．

本稿では，弾性線維に異常をきたす疾患の中で，弾性線維性仮性黄色腫について述べる．今回「展望」を書く機会をいただいたので，最近行った全国規模の調査[1]からみえた現時点での実態を紹介し，皮膚科医師の役割を述べる．

Ⅰ．弾性線維性仮性黄色腫

弾性線維は，膠原線維とは無関係に独立して存在する真皮ECMの代表の1つである．弾性が必要な血管，網膜などの器官に豊富に存在する．ヘマトキシリン－エオジンでは染色されず，elastica-van Gieson染色で黒く染まる．弾性線維はフィブリリン1，LTBPsなどを含む線維性成分であるマイクロフィブリルと，無構造のエラスチン分子の複合体である．エラスチン分子はその特徴的な分子内疎水結合ならびに分子内・間架橋により外力から解き放たれた際の復元(弾性)に大きく関わっている．弾性線維減少・機能不全により弾性を失った皮膚は，皺が目立つ，垂れ下がるといった症状を呈する．

1．弾性線維性仮性黄色腫(pseudoxanthoma elasticum：PXE)

ABCC6(ATP-binding cassette sub-family C member 6)遺伝子によりコードされる膜輸送蛋白質MRP6異常が原因で劣性遺伝形式をとって発症する．弾性線維の変性とカルシウム沈着が生じる．そのため皮膚真皮，粘膜，網膜基底膜(Bruch膜)，血管(血管壁弾性線維板)に障害がおこる．*ABCC6*遺伝子異常が発見されて12年以上経つが，弾性線維の変性・石灰化に至る経路は現時点でも不明で

*Utani, Atsushi(教授)　長崎大学大学院医歯薬学総合研究科皮膚病態学(〒852-8501 長崎市坂本1－7－1)

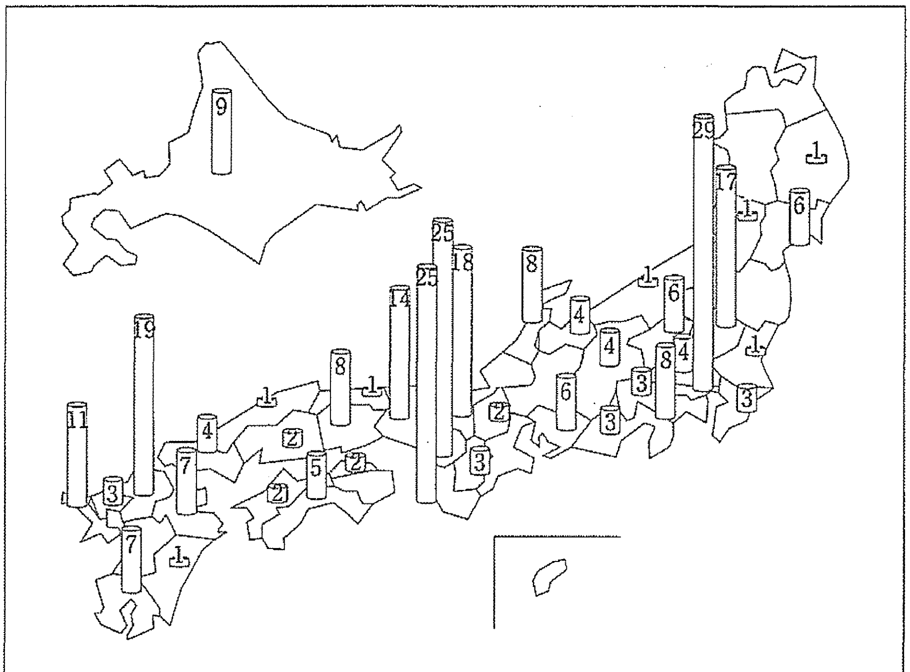

図1　都道府県別PXE　272例

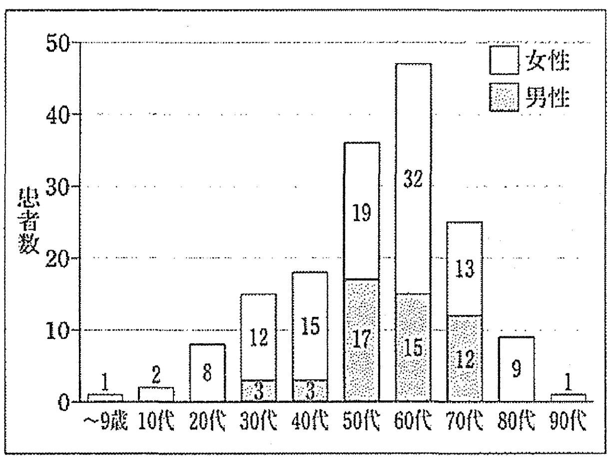

図2　年代別の症例報告数　162例

ある．

皮膚症状の初発が，眼，心血管障害の発症より若いため，患者は皮膚科を初診する可能性が高い．本疾患は皮膚科医がはじめに診断を下し，全身臓器の精査により病変を早期に発見するための指導的役割を果たし，患者のQOLを向上させうる疾患の1つである．

PXEは，臨床症状の重症度が不均一であり，同一家族内でもかなりの差があることが知られていた．そこで本邦の患者把握の必要性を考え，全国規模の実態調査を初めて行った(図1)． 方法は，全国大学・公立など主要病院の循環器科・眼科・皮膚科あわせて2,037科長にアンケートハガキを出し，1,098通の回答を得た．そのうち症例ありの106科(皮膚科からの回答が非常に多くを占めた)と，これに京大皮膚科，長崎大皮膚科を加えた108科の延べ272例であった．計算上は，全国では47万人に1名，長崎県だけをみると14万人に1名と多くの患者を発見することができた．

上のアンケートの患者の中で詳しく調査できた症例と，長崎大学皮膚科ホームページを介して登録した患者を合わせると，162例のデータ集計が終了した．年代別の症例報告数をみると平均57.2歳であり，中年以降に皮膚，眼，心・血管等の傷害で受診していることがわかる(図2)．受診時の各臓器別で異常・有病率をみてみると，皮膚科，眼科，循環器科という順であった(表1)．

次に，疾患の実態について詳しく述べていく．

a. 皮　膚　皮疹は，10～20代に発症のピークがある(図3)．黄色丘疹が線状，網目状にとくに頸部，腋窩，肘，臍周囲，鼠径部，膝窩，口腔粘膜などに多く出現し，太い皺にみえる場合もある(図4)．その頻度は記載があるものの中では96％(150/157)である．診断の第一は，とにかく全身をみることと，とくに頸部は95％，腋窩には66％の患者に認められるため，まずここの部位を丹念に探すことが重要である(表2，図5)．無疹症例が162例の中で7症例ある．

病理検査　組織検査の真皮中下層で弾性線維に変性・石灰化が認められる．とくに石灰化は，他

表1 受診時 各臓器別疾患有病率 162例

	記載あり		記載なし
症状	あり	なし	
皮膚科	150	7	5
眼科	126	11	25
循環器	86	56	20

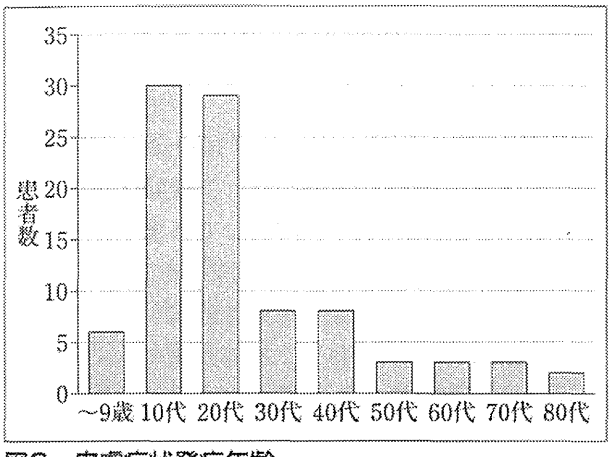

図3 皮膚症状発症年齢

図4 側頸部 皮疹

の皮膚症状が類似している疾患との鑑別に必須である．162例のうち130例(80%)で検査を行っていたが，そのうち95%の患者で弾性線維の異常がみつかっている．軽症，早期はH-E染色のみでは，弾性線維の変化がみつけにくいこともあるので，EVG染色，von Kossa染色を組み合わせることが重要となる．全体の4%にあたる皮疹のない7症例

表2 皮膚粘膜病変の部位 162例

		あり	なし	未検 記載なし
皮膚粘膜病変		150	8	4
皮膚病変	頸部	136	18	8
	腋窩	105	46	11
	鼠径部	78	71	13
	臍部	61	89	12
	肘窩	53	95	14
	膝窩	30	109	23
粘膜病変	口腔粘膜	29	111	22

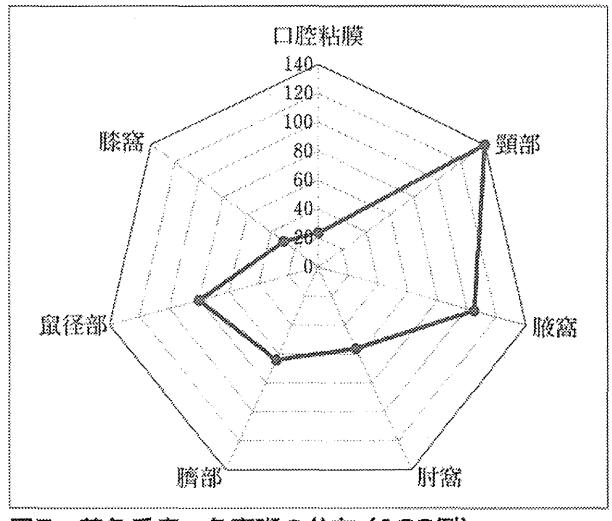

図5 黄色丘疹・色素斑の分布（162例）

は，すべてで弾性線維変性が同定できたため，診断には，皮膚症状と並んで組織の陽性所見が診断に重要である(診断基準参照)．

b. 眼 眼障害は，患者QOLに重大な影響を与えるものである．今回の全国調査では，記載のある患者の92% (126/137) の患者に，なんらかの検査異常，組織障害が認められる(表1)．患者は中年以降とくに50代にピークがある(図6)．

網膜基底膜(Bruch膜)の弾性線維が変性し脆弱となるためそこに亀裂がおこり，眼底に網膜血管様線条，オレンジ皮様外観を生じる．今回の調査では，記載のある患者の89% (119/133) に網膜血管様線条，74% (52/70) にオレンジ皮様外観が認められた(図7)．引き続き，眼底出血(67%；60/90)，脈絡膜新生血管(57%；50/87) が発生し

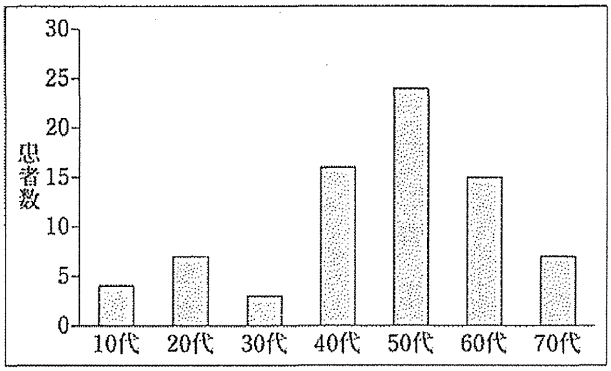

図6　眼科症状の発症時期

視力低下を生じるが，この2つは他疾患でも生じうるため特異性は低い．

視力障害　新聞を読むためには矯正視力で0.3以上は必要と考えられるが，矯正視力が測定できた症例(右110例，左108例)のうち，新生血管発症例43例に限ると平均矯正視力は小数視力0.3相当であった．　約50％で0.7以上の視力があった反面，30％で0.3未満の視力に低下していた．このことは眼症状発症前の視力は比較的良好であるが，いったん視力低下が始まると日常生活が困難な状態に低下する危険性を示している．

c. 心臓・血管　動脈壁中膜の弾性線維に変性・石灰化が生じ，動脈内腔が狭窄をおこす．今回の全国調査では，循環器障害は記載のある患者の60％ (86/132) に認められ(表1)，とくに高血圧は33％ (37/111) と非常に高い頻度でみられた．高血圧を除いた，脳梗塞，狭心症，間歇跛行，心筋梗塞，無症候性心筋虚血の頻度を示す(図8)．中年以降に発症する傾向があり，いずれの疾患も患者年齢平均51～54歳であった．

虚血性心疾患　年齢分布を示す(図9)．平成20年の厚生労働省の患者調査では，心虚血は50歳以上での有病率は1,000人あたりおよそ14人(1.4％) であるが，PXE患者では，13％ (17/132人) なので有病率は約10倍といえる．

脳血管障害　年齢分布を示す(図10)．平成20年の厚生労働省の患者調査では，50歳以上での有病率は1,000人あたり38人(3.8％) であるが，PXE患者では，10％ (13/140人) なので約2.6である．

この心臓，脳の虚血性疾患とも20～40代で発症するPXE患者が存在することは注意しなくてはならず，適切な医療により予防することが重要と考えられる．

2. 皮疹スコア：Dermscore

PXE皮疹の非連続性分布に着目し，皮疹分布部位(頸部，腋窩，鼠径部，肘窩，臍周囲)，口腔粘膜疹ごとに病変の「あり，なし」で，それぞれ1点，0点とし，合計6点とした[2]．その結果，皮疹スコアと口腔粘膜疹の存在が，循環器疾患の有病率と相関するという結果が出た．そのため，皮疹スコアが高い患者，口腔粘膜疹がある患者には積極的に検査・治療を進めるべきである．以前筆者はPXE患者15例による解析[2]を報告したが，それと同じ結果が今回の162例でも確かめられた．

3. 遺伝子解析

DNAシーケンスが終了したものは54例である．その内訳は，11例で変異なし，19例で1つの変異，24例で2つの変異を同定した．　同定率は62％であるが，欧米のそれと近い値である．変異部は18個であり，欧米とは異なる部位のものがほとんどである．複数患者に同じ変異が同定でき，創始者効果を認めた．ナンセン

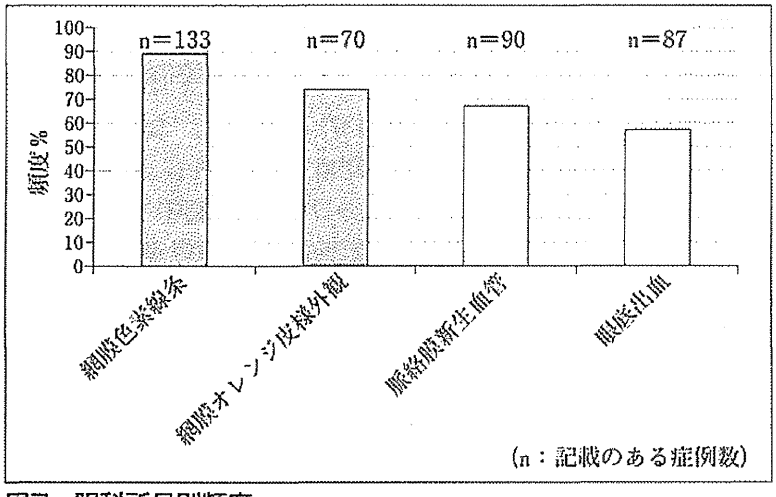

図7　眼科所見別頻度

ス変異による完全欠損例でも他のミスセンス変異と比べて重篤な臓器障害を合併しているということはなく，欧米と同じく日本においても遺伝子変異と臨床重症度，臨床型の相関性はなかった．MRP6変異による未同定の基質のわずかな減少が弾性線維そのものではなく，弾性線維の維持・保全に必須の因子に長年の経過で重大な機能不全を招くというPXEの代謝性疾患仮説[3]に関係していると考えられる．

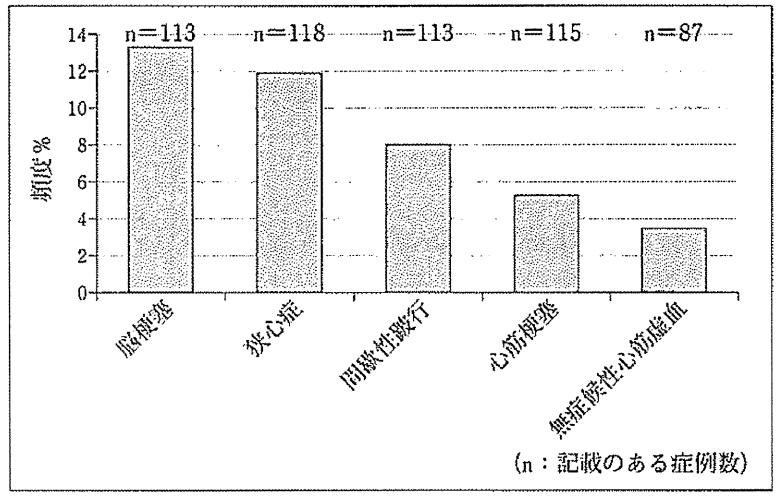

図8　虚血性疾患有病率

まとめ

PXEの全国調査を通して，初めて本邦の患者の実態が明らかになった．3大症状である皮膚症状，視力低下，虚血性疾患はいずれも発症後は対症療法しかないのが現状である．しかし網膜出血への早期治療，虚血性疾患の予防は患者QOLの低下を防ぐために有用と考えられ，皮膚科医は診断を早期に確定させるためにも関係各科と連携する主導的役割を担うべきと考える．遺伝子変異同定は，われわれの決めた診断基準では補助的な扱いにしているが，類似疾患との鑑別に有用である．遺伝子診断に関する問い合わせは，長崎大学皮膚科ホームページを参照していただきたい．　http://www.med.nagasaki-u.ac.jp/dermtlgy/

診断基準は，厚生労働省難治性疾患克服研究事業「弾性線維性仮性黄色腫の病態把握ならびに診断基準作成」班として2012年に診断基準を提案し，日本皮膚科学会雑誌[4]と日本眼科学会雑誌に掲載

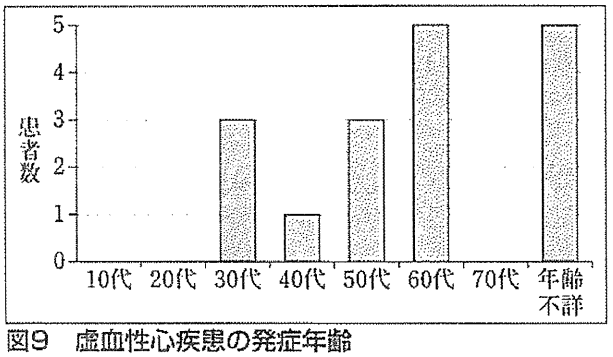

図9　虚血性心疾患の発症年齢

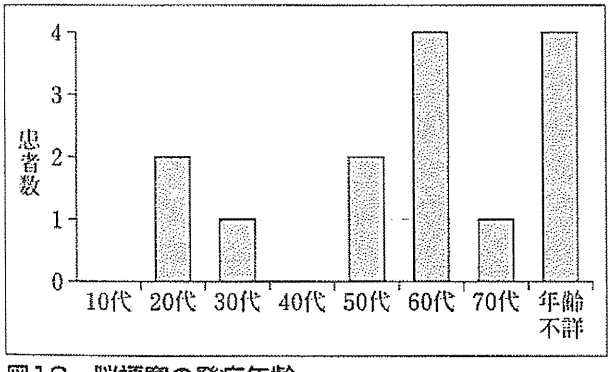

図10　脳梗塞の発症年齢

表3　皮疹スコア(dermcount (DC))と循環器疾患(CVD)有病率との相関

a)高血圧を含む

CVD	PXE症例数	DCの平均	SE
なし	68	2.03	0.195
あり	95	3.23	0.172

Two-sample Wilcoxon rank-sum (Mann-Whitney) test
p<0.0001

b)高血圧を除く

CVD	PXE症例数	DCの平均	SE
なし	85	2.2	0.17
あり	78	3.3	0.2

Two-sample Wilcoxon rank-sum (Mann-Whitney) test
p<0.0001

した．ここにその抜粋を紹介する．

弾性線維性仮性黄色腫診断基準　2012

A．診断項目
① 皮膚病変がある
② 皮膚病理検査で弾性線維石灰化をともなう変性がある
③ 網膜色素線条がある
④ *ABCC6*遺伝子変異がある

B．診断
Ⅰ．確診：(①または②)かつ ③
Ⅱ．疑診：(①または②)のみ，③のみ
注意：疑診例に④遺伝子変異を証明できた場合は，確実とする．

皮膚病変　10～20代で頸部，腋窩，鼠径部，肘窩，膝窩，臍周囲に好発する集簇性または線条に分布する黄白色丘疹で，癒合して局面となる場合もある．口唇粘膜に黄白色斑が認められる．典型的皮疹は見慣れた皮膚科医師には診断は容易であるが，皮疹を見慣れていない場合，また非典型皮疹のみの場合は，必ず組織検査を併用しなければならない．

病理像　皮疹のある部位から組織検査を行う．H-E染色で，真皮中層～下層に好塩基性に染色される石灰沈着を伴う変性弾性線維を認める．von Kossa染色等で石灰沈着を証明することは早期病変の診断ならびに鑑別診断に有用である．皮疹がない場合は，ブラインドで頸部，腋窩など好発部位より組織検査を行い，石灰沈着をvon Kossa染色等で証明する．

<文　献>
1) 研究代表者　宇谷厚志ほか．：厚生労働科学研究費補助金難治性疾患克服研究事業「弾性線維性仮性黄色腫の病態把握ならびに診断基準作成」平成24年度総括・分担研究報告書：2013
2) Utani, A. et al.：J Dermatol　37：130, 2010
3) Uitto, J. et al.：J Invest Dermatol　130：661, 2010
4) 宇谷厚志ほか：日皮会誌　122：2303, 2012

しわ 誤診？ 本当は 弾性線維性仮性黄色腫

長崎大学大学院医歯薬学総合研究科皮膚病態学　宇谷厚志

誤診されやすい背景

自覚症状のない薄い黄白色の皮疹であり，しわが太くみえる程度で，本人さえ気にしないこともある．しかしよく眼を懲らしてみると，黄白色扁平丘疹を見出せる場合や，正常とは違う異常に太いしわとして見出せる．